Structural Design of a Cathode-ray Tube (CRT) to Improve its Mechanical Shockproof Character

Sang Hu Park
Department of Mechanical Engineering, KAIST, Daejeon 305-701, Korea
Won Jin Kim*
School of Mechanical and Automotive Engineering, Keimyung University, 1000, Shindang-dong, Dalseo-gu, Taegu 704-701, Korea

An electronic beam mis-landing phenomenon on the RGB (red/green/blue)-fluorescent surface has been considered as one of serious problems to be solved in cathode-ray tube (CRT), which is generally caused by mechanical shock and vibration. In this work, structural design concepts on the major parts of the CRT, such as a frame, a shadow mask, and a spring, are studied to improve the mechanical shockproof character of a CRT by FEM-analyses and experimental approaches ; a frame is newly designed to have strength employing the double-corner-beads which reduces considerably the distortion of the frame and the shadow mask ; the edge-bead of a shadow-mask is redesigned to maintain the wide curved surface of a shadow-mask after mechanical shock ; finally, a spring supporting the frame and the shadow-mask is designed to have enough flexibility along drop-direction. As an example, a conventional type of a 15-inch CRT was utilized to demonstrate the feasibility and usefulness of this work. Overall, some favorable information on the structural design of the CRT is achieved, and the mechanical shockproof character of a 15-inch CRT is improved in the degree of 3 G (1 G=9.81 m/s^2) as an average-value.

Key Words : Cathode-ray Tube (CRT), Mechanical Shock, Modal Analysis, Finite Element Analysis

1. Introduction

The best products should have an ability to keep up not only their efficiency in working conditions but also reliability in the transporting conditions : by train, ship, truck, and airplane. To date, the cathode-ray tube (CRT) has been utilized widely as a monitor or a television set with a cheap price. However, for the large amounts of shipping, the volume of its package has been required to be reduced less and less. This indicates that the possibility of trouble-outbreak increases largely due to the simple package. Therefore, the shockproof character of a CRT in itself becomes an important issue. Generally, it is demanded that a CRT has special properties for transportation, and those are usually defined as product specifications. Among them, the mechanical shockproof character of a CRT is considered as a fundamental requirement to guarantee no troubles in transportation conditions. Until now, many industrial engineers have attempted to improve the mechanical characteristics of a CRT (Kim et al., 1998 ; 2000 ; 2003 ; Kim and Im, 1993 ; Ha et al., 2000 ; Ueyama et al., 1989 ; Baik et al., 1996 ; Kim and Park, 2003 ; Kim, 2003 ; You et al., 2000). Most of research

* Corresponding Author,
E-mail : wjkim@kmu.ac.kr
TEL : +82-53-580-5165; **FAX** : +82-53-580-5265
School of Mechanical and Automotive Engineering, Keimyung University, 1000, Shindang-dong, Dalseo-gu, Taegu 704-701, Korea. (Manuscript **Received** November 28, 2005; **Revised** June 3, 2006)

works have focused their efforts on solving the problems of a beam-landing-shift phenomenon occurring in operation due to the thermal expansion of the inner parts in the CRT. Some other works (Kim et al., 2000 ; 2003 ; Kim, 2003 ; You et al., 2000) have been conducted to improve the effectiveness of the howling-proof characteristic of a CRT employing various schemes. However, there are not enough available reports relating to the improvement of mechanical characters of a CRT ; what is worse, many works among them have been conducted inside each CRT-maker itself without any report for outside, on the base of empirical approaches or simple experiments. Therefore, it is not easy to figure out exactly the shockproof design concepts and to find out the dominant factors among the design parameters of a CRT. Ha et al.(2000) proposed a new experimental method to investigate the design parameters easily, and also they showed the comparison of the experimental and simulation results. Kim and Park (2003) proposed a new frame to increase its strength for the shockproof character of a CRT.

Figure 1 shows the schematic structure of a conventional 15-inch CRT : a shadow-mask, a frame, a spring, and many other parts. Among them, the shadow-mask is considered as the most important part, because the quality and resolution of screen image is determined by the characteristics of a shadow-mask, including its curvature and the size and shape of beam-guiding holes on its surface. A shadow-mask is usually made of a thin invar (Fe-36Ni) sheet (about 0.1～0.12 mm in thickness) to reduce its thermal expansion ; therefore, plastic deformation on the shadow mask can occur readily by mechanical shock from the outside. Therefore, it is required necessarily that a shadow-mask has enough robustness itself. If the shadow-mask is damaged slightly by an external force, it can not play the important role to guide electronic beams onto exact positions of the RGB-fluorescent units, of which a phenomenon is defined as the mis-landing of electrons. Figure 2 shows an example of the mis-landing phenomenon induced by the damaged shadow-mask after a mechanical drop. This phenomenon occurs readily when a CRT is dropped along the weakest drop direction, which is known as the backward direction of the CRT from the panel to the funnel (see the arrow mark in Fig. 1). In recent years, flat-and-wide CRTs are rapidly increased in order to enhance the quality of image ; therefore, a shadow-mask should have a very large radius of curvature, which causes the reduction of structural strength. Moreover, most buyers of a CRT

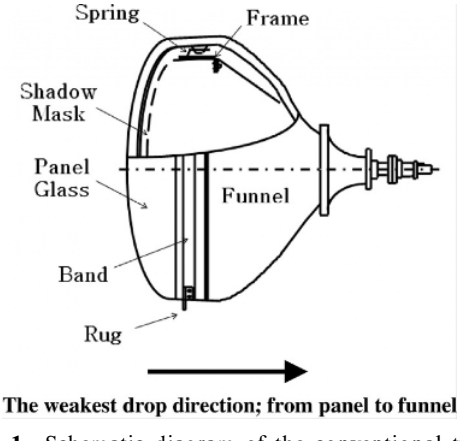

Fig. 1 Schematic diagram of the conventional type of a CRT which consists of the frame, the shadow mask, the spring, panel/funnel glass, and so on. The arrow indicates the weakest drop direction ; from panel glass to funnel glass

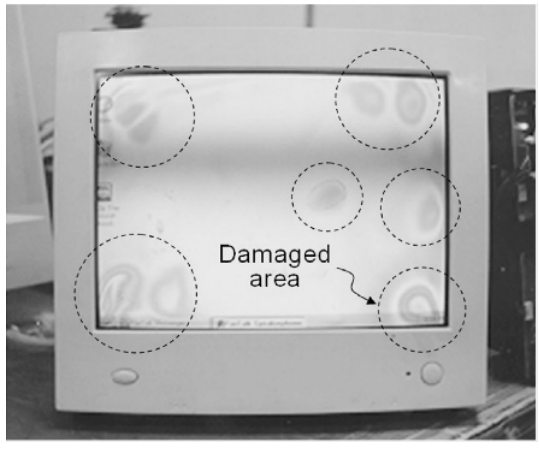

Fig. 2 Photograph of electron mis-landing phenomenon due to deformed shadow mask after mechanical shock test

increase gradually the degree of shockproof characteristics of a CRT for worldwide distribution. In this work, the design concepts of major parts in a CRT are proposed for the improvement of shockproof characteristic of a CRT.

2. Shockproof Design of the Structures Using Modal Analysis

2.1 Improvement of strength of the shadow-mask and the frame

As above-mentioned, the shadow-mask has an important role to guide electrons emitted from an electron gun into exact positions of the RGB (red/green/blue)-fluorescent cells on a screen area. Therefore, it needs to have enough strength to prevent plastic deformation and howling motion under mechanical shock and vibration. Typical design approaches for improving strength of a shadow-mask are the followings; (i) controlling the curvature of the shadow mask, by reason that a high curvature of a shadow-mask gives high strength; (ii) making suitable edge-beads; (iii) heat treatment or coating some hard material on the surface of a shadow-mask for increasing hardness, which is a simple and easy way, but it requires additional cost. The frame supporting the shadow-mask robustly is also an important part to reduce deformation and vibration of the shadow-mask. In case the frame is distorted more than somewhat degree, plastic deformation may occur on the shadow-mask. In order to increase strength of the frame and the shadow-mask effectively, in this work, a method of designing suitable beads is redesigned using a modal analysis method.

For improving strength of the shadow-mask, two feasible edge-beads; v-groove-bead and step-bead, were designed and considered. The inserts of Fig. 3(a) illustrate schematically the dimensions of each designed edge-bead, which is the largest dimension in size considering its design specification and formability of a metal-forming process. However, it is difficult to analyze explicitly the vibration modes of the shadow-mask employing experimental methods, because the shadow-mask is too thin to keep its initial conditions; for instance, shape and curvature, during the modal

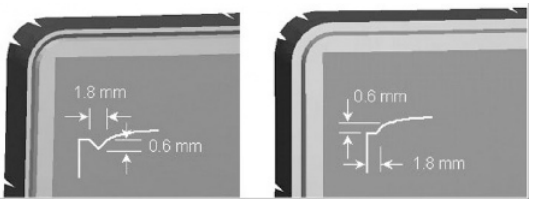

(a)

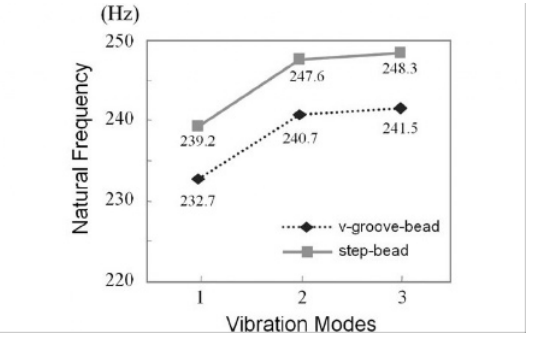

(b)

Fig. 3 (a) Schematic part diagrams of the shadow mask with each edge-bead shape; v-groove-bead (left) and step-bead (right). (b) Comparison of the modal analysis results between the shadow masks

tests. So, we have attempted to evaluate the modal shapes numerically using I-DEAS (2004) with consideration of material properties. Figure 3(b) shows the comparison of natural frequencies of the shadow-mask in case of two different edge-beads used. From the results of modal analyses, it is clear that the step-bead is much superior to the v-groove-bead; whose natural frequency is much higher as 6.7 Hz. This means that the shockproof characteristic of a CRT can be improved, when a shadow-mask involving the step-bead is used.

In order to achieve some information on improving strength of the frame, an experimental modal analysis of the frame under a free-free condition has been carried out. Figures 4(a) and 4(b) show the schematic diagram of an experimental setup for the modal analysis. It is well-known that low-level modes such as 1st and the 2nd mode are of interest modes in the drop and shock problems, because the propagation energy in higher modes is low, and decays rapidly; therefore, the shock energy in higher modes seldom has influence on large deformation of the frame. In

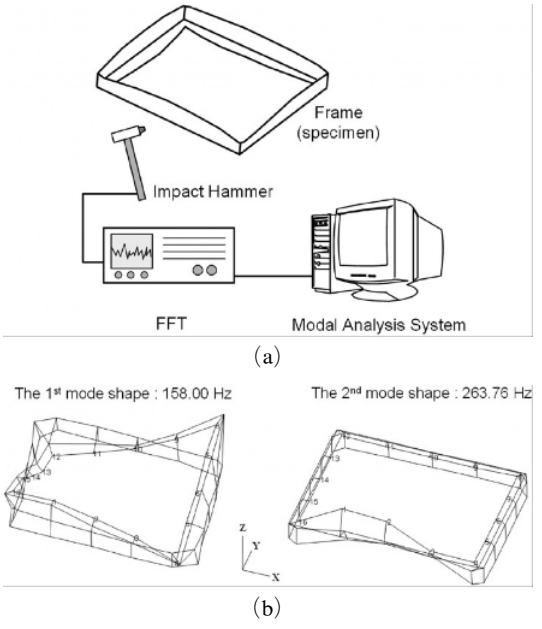

Fig. 4 (a) Schematic diagram of experimental apparatus for modal analysis and (b) the 1st and the 2nd mode shapes of the present frame

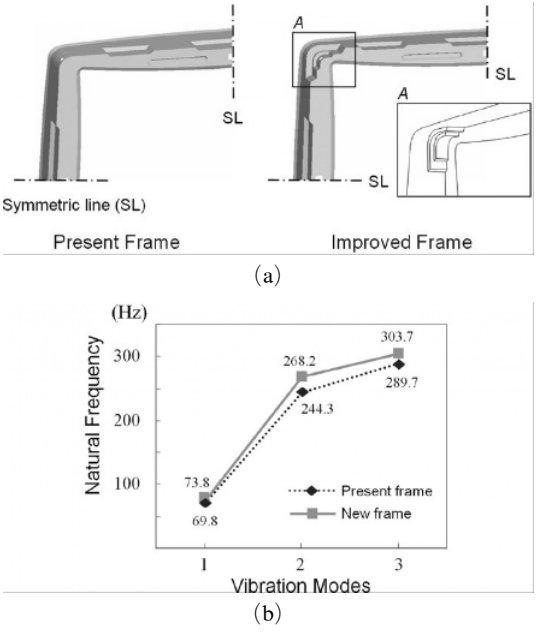

Fig. 5 (a) Comparison of the present frame and the newly designed frame; an inner box shows the schematic diagram of the corner shape of the new frame. (b) The results of experimental modal test of the two frame

the 1st and 2nd modes of the original frame (which has no corner-beads), twist modes have appeared dominantly, as shown in Fig. 4(b), which result in the deformation of the shadow-mask. Therefore, the frame needs to be reinforced with strong corner-beads to reduce twist-deformation after mechanical shock. By these reasons, a novel frame with double-corner-beads on its four corners was proposed to have a resistance against the mode of twist-deformation. Figure 5(a) shows the comparison of the original frame with the modified frame (corner part in full shape). In order to increase the effect of corner-bead, the size of beads was designed large considering the design specifications. In Fig. 5(b), the variation of natural frequencies between the original and modified frames is shown. The increase of natural frequency was 4 Hz at the 1st mode and 23.9 Hz at the 2nd mode, respectively. From the results, we demonstrate clearly the efficiency of double-corner-bead.

2.2 The flexible twisting spring (T-Spring)

A spring used in the CRT has two important roles; one is to support the frame firmly for the stable fabrication process of a CRT (especially, in deposition process of the fluorescent RGB dyes), and for preventing the howling problem; the other role of a spring is related to the mechanical shockproof characteristic, which is firstly demonstrated in this work. To date, most engineers have considered only the former function in the design of a spring; therefore, the spring has been designed to be very strong until now. However, in case the springs have ability to absorb the shock energy to somewhat degree, the propagating shock energy into the frame and the shadow-mask can be reduced dramatically. Therefore, we can expect the improvement of shockproof characteristics of the CRT via the absorbing mechanism. An ideal spring has two independent peculiarities along two directions; insertion-direction and drop-direction (see Figs. 6(a) and 6(b)). A spring should have stiffness along the insertion-direction into the panel glass, and should have the flexibility along the drop-direction to absorb

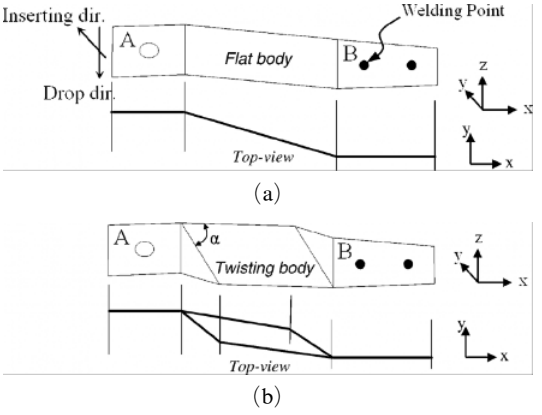

Fig. 6 (a) Schematic view of the present spring shape that has a flat body and ends, and (b) the newly designed twisting spring (T-spring) that has a twisting body and flat ends

shock energy. However, the original spring (Fig. 6(a)), which has been widely used as a conventional CRT spring, consists of a flat body and flat ends, so it has stiffness along the both directions due to its morphological shape. In case the thickness of the present spring is reduced to increase its flexibility along the drop-direction, it cannot play a role to support the frame strongly along the insertion-direction; this condition is called as a contradiction. In order to have two peculiarities depending on the two directions, twisting spring (T-spring) which is contrived to be a twisting body and flat ends, as shown in Fig. 6(b), is proposed. The twist angle (α) is reasonable in range of 45° to 60°. We have attempted finite-element-(FE) analyses to evaluate the flexibility of T-spring comparing the original spring: analysis model (Fig. 7(a)) and simulation results (Fig. 7(b) and 7(c)). In the analysis model, the both ends of the frame are fixed and the springs were joined to the frame by two spot-welding points. Then, a static force of 10 kgf was loaded at the center point of the insertion hole. The results show that deformation of the T-spring is much larger than that of the original spring in degree of 6.44% along the z-axis (drop-direction). Moreover, the frame is not affected by the deformation of T-spring, which is known as one of causes for deforming the shadow-mask.

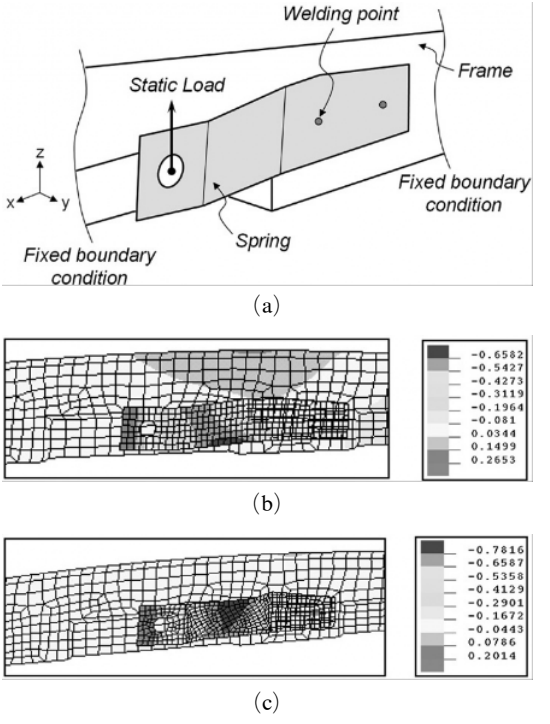

Fig. 7 A simple model for analyzing deformation of each spring, and the comparison of the simulation results of deformation distribution along z-axis in case of (b) the present spring and (c) the T-spring (units: mm)

3. Mechanical Drop Simulations of the CRT

3.1 Effective material properties of shadow-mask

We have tried to demonstrate the effects of newly designed T-spring, frame, and shadow-mask using the FE method. However, it is difficult to measure directly the material properties of a shadow-mask using the general tensile test due to numerous holes on the mask. In order to calculate the effective material properties of the shadow mask for use in the simulation, an analytical approach has been carried out, as shown in Figs. 8(a) to 8(c). The inside holes on the shadow-mask have some rules in their arrays, shapes, and sizes which are determined by design specifications. However, it is almost impossible to analyze the full shadow-mask model considering the whole arrays of holes with their detailed dimensions,

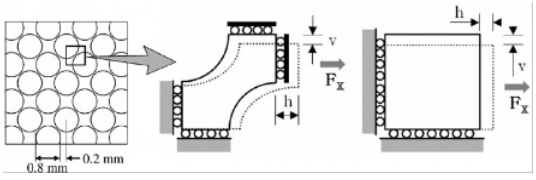

Fig. 8 Bold lines shows undeformed shape of the analysis model and the dotted line is the deformed shape; (a) schematic diagram of the section of the shadow mask, (b) unit-cell model of the shadow mask, and (c) the equivalent continuum plate model

because the full model of holes causes to generate too many elements in the FE analysis. Therefore, it is more useful method to employ the effective properties of the shadow-mask in the FE-analysis. As illustrated in the Fig. 8(c), a rectangular plate without holes, which is the same size of a unit cell model (Fig. 8(b)), is introduced to calculate the effective material properties. The unit cell model represents the real geometric dimensions and boundary conditions of the holes to be deformed analogously along the direction of x-axis and y-axis. The main idea of this scheme is that the elastically deformed shape of a small rectangular element in a large continuum plate maintains its rectangular shape by the constraints of boundary conditions, when symmetric forces are imposed along x-axis and y-axis in the plate. This deformation character can be applied identically as the boundary conditions of the unit cell model to obtain the effective material properties. The effective properties of the x-axis and the y-axis are calculated by applying the following equations (1) to (4);

$$E_x=\frac{\sigma_x}{\varepsilon_x}=\left(\frac{F_x}{dy\cdot dz}\right)\Big/\left(\frac{h}{dx}\right) \tag{1}$$

$$E_y=\frac{\sigma_y}{\varepsilon_y}=\left(\frac{F_y}{dx\cdot dz}\right)\Big/\left(\frac{v}{dy}\right) \tag{2}$$

$$P_{yx}=\frac{\varepsilon_y}{\varepsilon_x}=\left(\frac{v}{dy}\right)\Big/\left(\frac{h}{dx}\right) \tag{3}$$

$$P_{xy}=\frac{\varepsilon_x}{\varepsilon_y}=\left(\frac{h}{dx}\right)\Big/\left(\frac{v}{dy}\right) \tag{4}$$

Table 1 Comparison between original and effective material properties of the shadow-mask

	Original Properties (A)	Effective Properties (B)	Ratio (B/A)%
E_x, E_y (N/mm^2)	2.1×10^5	1.2×10^4	5.7
p_{yx}, p_{xy}	0.3	0.41	137
Density (kg/mm^3)	7.80×10^{-6}	5.21×10^{-6}	66.8

where the subscripts x and y represent the x-axis and y-axis respectively; E is the Young's modulus, p is the Poisson ratio, and σ is the normal stress; ε and γ are the normal and shear strains; dx, dy, and dz are the initial element dimensions of the unit-cell-model in the x, y, and z-axis; h and v are the deformations of the unit cell model in the x-axis and y-axis due to the loadings of $\mathbf{F}_x$ and $\mathbf{F}_y$.

In Table 1, the comparisons of the original invar plate properties and the effective properties calculated from the unit cell model are summarized. The effective elastic modulus of the shadow mask is only 5.7% rate comparing with that of the continuum invar plate, and the effective material properties are the same values along x-axis and y-axis due to the symmetric shape of the holes.

3.2 Evaluation of shockproof characteristic using FE-analysis

The FE model of the CRT for the drop simulations was constructed with the major parts of the CRT: shadow-mask, frame, springs, and panel glass. In order to reduce computational time and effort, some engineering assumptions have been regarded as the followings; (i) a panel glass is assumed as a rigid body, because it is seldom deformed under mechanical shock in comparison with the other parts; (ii) the funnel glass is omitted in the analysis model owing to its rigidity but its mass was added into the center of gravity of the panel glass to consider the amounts of inertia forces of the CRT; (iii) the shock energy is perfectly delivered into the CRT without any loss term like friction and thermal loss energy. Figure 9(a) and 9(b) show the schematic and finite

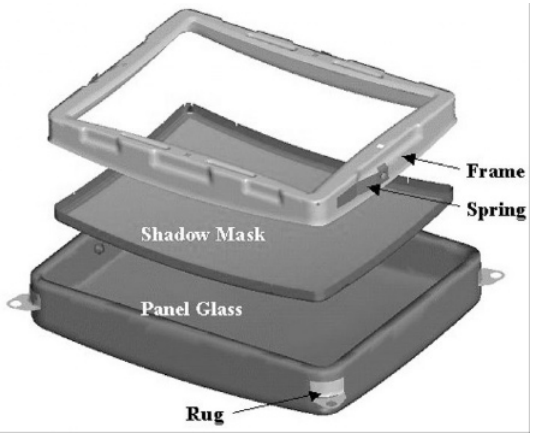

(a)

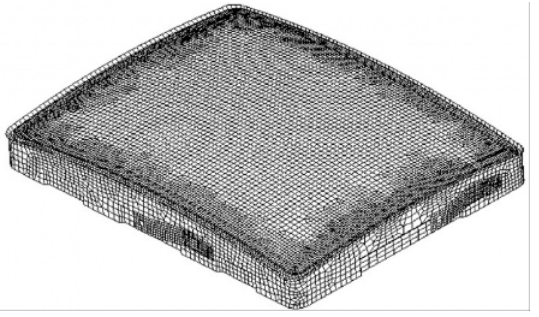

(b)

Fig. 9 (a) Analysis model in unassembled stat for explanation, and (b) the finite element model of major parts; the shadow-mask, the frame, and the springs

element model which consisted of 1,266 solid elements and 3,285 of shell elements for each part. The input velocity is obtained using the critical drop-height of a CRT. The critical height means a maximum endurance height without any visible defects on a CRT. For achieving the exact critical drop-height, we have constructed the shock-test equipment as shown in Figs. 10(a) and 10(b). Describing the procedure of the drop test briefly, a CRT is fixed firmly on a rigid mounting jig via screwing four rugs. Then, the jig is fastened tightly on the shock table using belts in order to translate shock energy perfectly from the table to the CRT. An accelerometer is installed on the shock table to acquire the time history of accelerometer depending on the drop height, and the duration time of shock is controlled by a cushioning pad

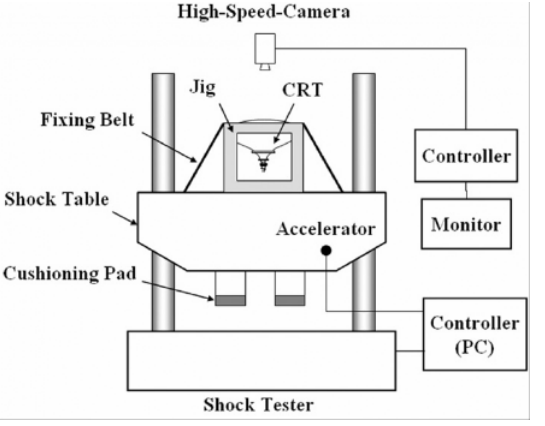

(a)

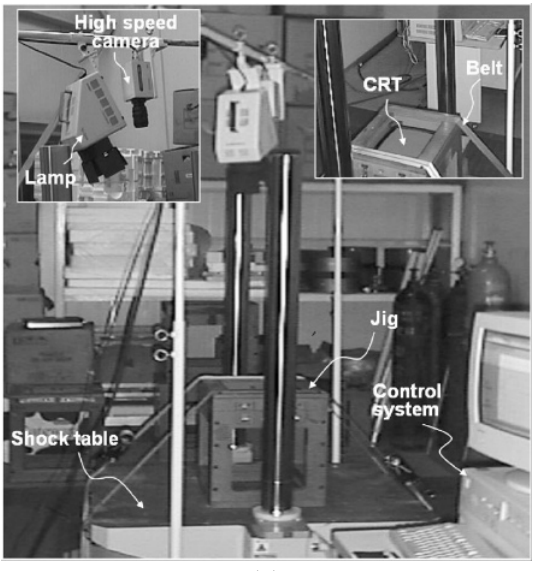

(b)

Fig. 10 (a) Schematic diagram of experimental apparatus for the drop-test of the CRT and (b) its photograph

(in this work, a pad for 10 ms duration was used). A high-speed-camera is used to monitoring some errors that can be broken out during the tests. In order to find out the critical drop height of the CRT accurately, drop tests have been conducted with three times iteratively at each drop-height, and the drop-height is increased gradually until visible damages occurred on the shadow mask. When plastic deformation occurs on the mask, some dim blotches, as shown in Fig. 2, can be detected easily by a naked-eye examination.

Generally, the critical acceleration at the critical drop height is defined as the shockproof character of the CRT. In this work, the critical drop height of the initial CRT model was 596.5 mm (in this height, the critical velocity is 3.421 m/s), and the average acceleration corresponding to the height was 40.3 G (1 G=9.81 m/s^2).

Three modified CRT test models, consisting of newly designed parts, have been constructed to evaluate their shockproof character as the followings;

(1) Model-I: It is made up of the step-bead shadow mask of 0.12 mm thickness, the original spring of 0.7 mm thickness, and the original frame of 1.2 mm thickness i.e., it was almost similar to the original CRT except the edge-bead shape of the shadow-mask

(2) Model-II: It consists of the step-bead shadow mask of 0.12 mm thickness, the double-corner-bead frame of 1.2 mm thickness, and the T-spring of 0.7 mm thickness

(3) Model-III: The thickness of the shadow-mask is only changed to 0.1 mm in case of the second model, and the other things are identical.

The frame is inserted firmly in the panel glass by the springs into pins located inside of the panel. In the inserting process of the springs into the pins, the springs deformed elastically and have initial residual stresses to support the frame strongly. And it is well known that the deformed shapes and the residual stress distributions of the springs have much influence on deformation of the shadow-mask, when a CRT is dropped. Therefore, they have to be considered to get more accurate results of the drop simulations. In this work, a FE-analysis on the process of inserting pins into the panel glass has been carried out using an explicit FE-code (Pam-Crash User's Manuals, 2004) before drop simulations, and the results of residual stress and shape were reflected into the drop simulations as initial conditions. Figure 11(a) and 11(b) show the results of spring inserting process. Using the FE-model (see Fig. 9 (b)) with boundary conditions and material properties, we have done drop-simulations. In Figs. 12(a) to 12(c), the simulation results of the maximum deformation of the masks in each case are shown. Maximum deformation energies of each shadow mask from Model-I to Model-III are 8.2, 6.3 and 7.4 J, respectively. This means that the Model II has the best shockproof characteristic among the test models. Furthermore, the Model-III is analogous to the Model-II except the difference of thickness of the shadow-mask (1.2 mm in Model-II, 1.0 mm in Model-III), but the result is considerably different. From this, it is clear that the strength of the shadow mask is a much more sensitive parameter than the others. The Model-I is similar to the initial model of a CRT, and its locally deformed domains, as shown in Fig. 12 (a), are very analogous to the experimental result shown in Fig. 2.

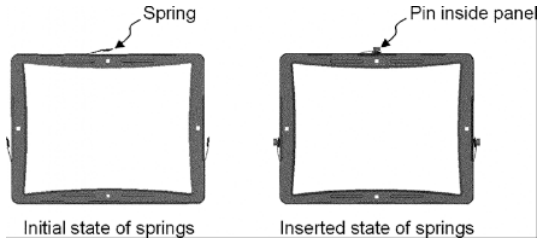

Fig. 11 (a) Initial state of the springs and the frame and (b) the deformed shape of the springs after inserting into the pins

Fig. 12 The deformed shape of each shadow mask; (a) the 1st model consisted of the new designed shadow mask of 0.12 mm in thickness, the present frame of 1.2 mm, and the present springs of 0.7 mm; (b) the 2nd model consisted of the new designed shadow mask of 0.1 mm in thickness, the new frame of 1.2 mm, and the T-springs of 0.7 mm; (c) the 3rd model consisted of the new shadow mask of 0.10 mm in thickness, the new frame of 1.2 mm, the T-springs of 0.7 mm. Deformation energy within the shadow mask of each case is described in Table 2

Table 1 Three modified CRT models and their experimental results

Types	Thickness (mm)			Experimental Results (Min./Ave./Max. of acceleration) (G)
	Frame	Shadow mask	Spring	
Model I	1.2(O)	0.12(N)	0.7(O)	42.0/44.4/46.8
Model II	1.2(N)	0.12(N)	0.7(N)	46.8/47.6/48.7
Model III	1.2(N)	0.10(N)	0.7(N)	39.6/41.6/44.4

*Notice : N is new design and O is old design

In order to demonstrate the simulation results, experimental drop tests (ASTM, 2000) of each model have been done. The tests were repeated 10 times for each model to obtain reliable data, and Table 2 summarizes the experimental layouts and their results, respectively. From the experiment results, the Model-II shows the best shockproof characteristic, as we have expected. The model has an increase of 3 G in average value comparing with the critical acceleration of the Model-I (which is similar to the initial CRT model) ; furthermore, its acceleration variation is also diminished. Therefore, the Model-II is demonstrated clearly to be an improved model with the narrow fluctuation of shockproof characteristic, and the proposed design concepts for frame, shadow-mask, and spring are very valuable.

4. Conclusions

In summary, the design concepts for the inner structures of a CRT : shadow-mask, frame, and spring, are proposed to improve the shockproof characteristic. The followings are what we come to conclusions on the design concepts : the frame and the shadow-mask have to be designed to have enough strength, and the spring needs to be designed to have the two different properties along insertion-direction and drop-direction. Two kinds of bead shape for increasing the strength of a shadow-mask : step-bead and v-groove-bead, have been considered. From the results of modal analysis, it is known that the step-bead is more effective. The frame with double-corner-beads has been proposed to enlarge its strength at the twist dominant modes : the 1st and the 2nd modes. The increase of natural frequency of the proposed frame was approximately 14 Hz in average comparing with the original frame which have no corner-beads. The T-spring consisting of one twisting body and two flat ends, has been devised firstly to have two different properties : deformability and stiffness, along two directions, respectively. We have attempted to evaluate the three modified CRTs mixing the newly designed components of a CRT. Through this work, we got an improved CRT whose critical acceleration is increased in the degree of 3 G comparing with that of the initial CRT model. Also, the proposed design concepts of the conventional CRT may be extended to design the flat and wide type of a CRT.

References

ASTM Code D3323-93 and D4169, 2000, *ASTM Testing Standards*, (American Society for Testing and Materials, Philadelphia, Pennsylvania).

Baik, S. C., Oh, K. H., and Lee, D. N., 1996, "Analysis of the Deformation of a Perforated Sheet Under Uni-axial Tension," *J. Mater. Proc. Techn.*, 58, pp. 139～144.

Ha, K., Kim, D. and In, J., 2000, "Prediction of CRT Shock Test and Design Improvement for Shock Resistance," *Int. Conf. of SID, Long Beach/CA/USA*, pp. 952～955.

I-DEAS 10 NX Series User's Manuals, 2004, (EDS).

Kim, H. G. and Im, S. Y., 1993, "Analysis of Beam Landing Shifts due to Thermal Deformation of a Shadow Mask," *IEEE Transaction on Consumer Electronics*, 40, pp. 47～54.

Kim, K. W., Kim, N. W. and Kang, D. J., 1998, "Analysis of Shadow-mask Thermal Deformation and Prediction of Beam Landing Shifts for Color CRT," *IEEE Trans. on Consumer Electronics*, 44, pp. 442～448.

Kim, S. D. and Park, S. H., 2003, "Frame for Color Cathode-ray Tube," *US Patent*, No. US6. 577.049.

Kim, S. D., 2003, "Nonlinear Vibration Analysis of Thin Perforated Sheet with Wire Impact

Damping," Ph.D. Thesis (Korea Advanced Institute of Science & Technology).

Kim, S. D., Kim, S. G., Seo, J. W. and Jeong, B. K., 2000, "Frame Structure for a Cathode-ray Tube," *US Patent*, No. US5.698.938.25.

Kim, S. D., Kim, W. J. and Lee, C. W., 2003, "Vibration Analysis of the Tension Shadow Mask with Wire Impact Damping," *J. Sound and Vibration*, 256, pp. 1003～1023.

Pam-Crash User's Manuals, 2004, (ESI Group).

Ueyama, T., Kanai, H., Hirai, R. and Yano, T., 1989, "Improved Computer Simulation Method for Shadow-mask Thermal Deformation and Beam Shift," *Japan Display*, 89, pp. 558～561.

You, S. J., Shin, W. S. and Jang, B. W., 2000, "An Analysis of a Mask Vibration Considering Contact with a Damping Wire," *IEEE Transactions on Consumer Electronics*, 46, pp. 385～389.